J|A|C|S
ARTICLES
Published on Web 02/06/2007

Effects of Gas Molecules on Nanofluidic Behaviors

Yu Qiao,[†] Guoxin Cao,[‡] and Xi Chen*,[‡]

Contribution from the Department of Structural Engineering, University of California at San Diego, La Jolla, California 92093-0085, and Department of Civil Engineering and Engineering Mechanics, Columbia University, New York, New York 10027-6699

Received October 6, 2006; E-mail: xichen@civil.columbia.edu

Abstract: Most previous studies on nanofluidic motions were focused on liquid−solid interactions, with the important role of gas phase being ignored. Through a molecular dynamics simulation, we show that the gas−liquid interaction can be an indispensable factor in nanoenvironments. Gas molecules in relatively large nanochannels can be dissolved in the liquid during pressure-induced infiltration, leading to the phenomenon of "nonoutflow". By contrast, gas molecules tend to form clusters in relatively small nanochannels, which triggers liquid defiltration at a reduced pressure. The results qualitatively fit with the observations in a high-pressure-resting experiment on nanoporous silica gels.

Introduction

Understanding behaviors of liquids in nanoenvironments is of important relevance to drug delivery, programmable catalysis, selective absorption, and energy-related applications, among others. For instance, as a nonwetting liquid is forced into an otherwise energetically unfavorable nanopore by applying an external pressure, the thermodynamic equilibrium at the liquid−solid interface can be directly controlled by mechanical methods. As a result, a significant portion of the work done by the external pressure is converted to the solid−liquid interfacial tension, and this structure can be used for developing high-performance energy absorption and control systems.[1]

The fundamental infiltration and defiltration mechanisms of nanofluidics are distinct from that of bulk phases, as analyzed by a number of molecular dynamics (MD) simulations in the past few years.[2] However, in most of these analyses, the liquid molecules were placed in vacuum nanotubes or nanochannels. For example, Hummer et al.[3] reported that a chain of water molecules could spontaneously enter and continuously exist in a carbon nanotube (CNT), resulting in water conduction, while the absolute vacuum condition in their simulations is difficult to achieve in real experiments. By embedding CNTs in a thin membrane, Holt et al.[4] were able to measure water or air flows through the nanotubes; however, neither gas nor liquid molecules were entrapped in the nanotubes, and such a system could not be used for energy absorption. Currently, the study on gas nanophase effects was focused on large liquid−solid interfaces for flow boundary condition analysis,[5] surface force measurement,[6] and gas solubility in water-filled nanopores.[7] Both computational and experimental investigations on the kinetics of gas−liquid−solid interactions in confining nanoenvironments are still lacking.

In a bulk liquid, the gas nanophase that typically consists of a few to several hundred gas molecules often has secondary influence on the liquid motion, in part due to the low gas molecule density that is usually a few orders of magnitude smaller than that of liquids. Thus, within a constant volume, the overall forces exerted on liquid by gas molecules are negligible, compared with liquid−liquid and liquid−solid interactions. In a nanochannel, however, due to the radial confinement the effective gas molecular density significantly increases. As the nanotube diameter is smaller than a few nanometers, a single gas molecule could make it difficult for the infiltrated liquid molecules to bypass it; thus, the gas molecule is analogous to a moveable "divider" which keeps liquid molecules on one side, and the gas molecule can also be pushed out of the way by the infiltrated liquid molecules. In our recent experimental study on nanoporous silica gels, as will be discussed in detail shortly, it was discovered that the liquid defiltration in nanopores of relatively high gas concentrations

[†] University of California at San Diego.
[‡] Columbia University.

(1) (a) Han, A.; Qiao, Y. *J. Am. Chem. Soc.* **2006**, *128*, 10348. (b) Kong, X.; Qiao, Y. *Appl. Phys. Lett.* **2005**, *86*, 151919. (c) Surani, F. B.; Kong, X.; Qiao, Y. *Appl. Phys. Lett.* **2005**, *87*, 163111. (d) Surani, F. B.; Kong, X.; Qiao, Y. *Appl. Phys. Lett.* **2005**, *87*, 251906. (e) Lefevre, B.; Saugey, A.; Barrat, J. L.; Bocquet, L.; Charlaix, E.; Gobin, P. F.; Vigier, G. *J. Chem. Phys.* **2004**, *120*, 4927.
(2) (a) Wasan, D. T.; Nikolov, A. D. *Nature* **2002**, *423*, 156. (b) Sansom, M. S. P.; Biggin, P. C. *Nature* **2001**, *414*, 156. (c) Majumder, M.; Chopra, N.; Andrews, R.; Hinds, B. J. *Nature* **2005**, *438*, 44. (d) Walther, J. H.; Jaffe, R.; Kotsalis, E. M.; Werder, T.; Halicioglu, T.; Koumoutsakos, P. *Carbon* **2004**, *42*, 1185. (e) Kalra, A.; Garde, S.; Hummer, G. *Proc. Natl. Acad. Sci. U.S.A.* **2003**, *100*, 10175. (f) Mann, D. J.; Halls, M. D. *Phys. Rev. Lett.* **2003**, *90*, 195503. (g) Zhu, F. Q.; Tajkhorshid, E.; Schulten, K. *Phys. Rev. Lett.* **2004**, *93*, 224501. (h) Wan, R. Z.; Li, J. Y.; Lu, H. J.; Fang, H. P. *J. Am. Chem. Soc.* **2005**, *127*, 7166. (i) Sriraman, S.; Kevrekidis, I. G.; Hummer, G. *Phys. Rev. Lett.* **2005**, *95*, 130603. (j) Zimmerli, U.; Gonnet, P. G.; Walther, J. H.; Koumoutsakos, P. *Nano Lett.* **2005**, *5*, 1017.
(3) Hummer, G.; Rasalah, J. G.; Noworyta, J. P. *Nature* **2001**, *414*, 188.
(4) Holt, J. K.; Park, H. G.; Wang, Y. M.; Stadermann, M.; Artyukhin, A. B.; Grigoropoulos, C. P.; Noy, A.; Bakajin, O. *Science* **2006**, *312*, 1034.
(5) (a) Granick, S.; Zhu, Y.; Lee, H. *Nat. Mater.* **2003**, *2*, 221. (b) Steitz, R.; Gutberlet, T.; Hauss, T.; Klösgen, B.; Krastev, R.; Schemmel, S.; Simonsen, A. C.; Findenegg, G. H. *Langmuir* **2003**, *19*, 2409. (c) Mezger, M.; Reichert, H.; Schöder, S.; Okasinski, J.; Schröder, H.; Dosch, H.; Palms, D.; Ralston, J.; Honkimäki, V. *Proc. Natl. Acad. Sci. U.S.A.* **2006**, *103*, 18401.
(6) (a) Meyer, E. E.; Lin, Q.; Israelachvili, J. N. *Langmuir* **2005**, *21*, 256. (b) Doshi, D. A.; Watkins, E. B.; Israelachvili, J. N.; Majewski, J. *Proc. Natl. Acad. Sci. U.S.A.* **2005**, *102*, 9458.
(7) Luzar, A.; Bratko, D. *J. Phys. Chem. B* **2005**, *109*, 25545.

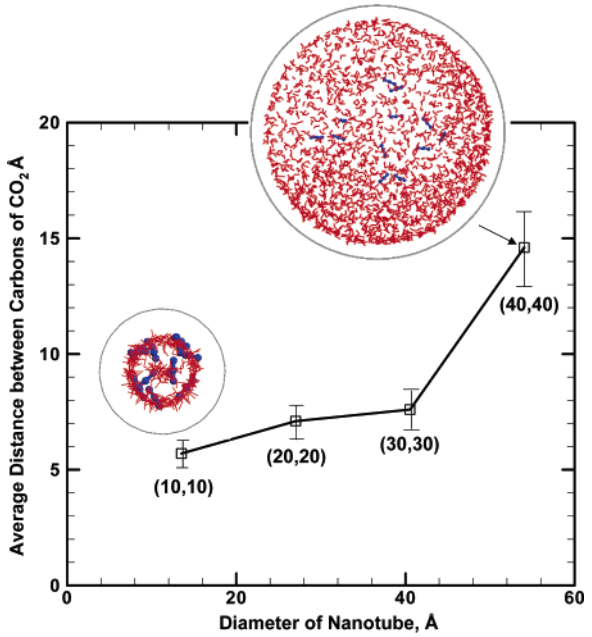

Figure 1. Gas solubility study showing the average distance between the nearest carbon atoms in CO_2 molecules as a function of the nanopore radius. The insets show snapshots at 20 ps: in the smaller (10,10) tube the gas molecules form a cluster, whereas the gas molecules were quickly dissolved in a larger (40,40) tube. The water molecules were in red, and the CO_2 molecules were in blue.

was much easier than in nanopores of relatively low gas concentrations. In the current study, through an MD simulation, we show that the mass and energy exchange between gas and liquid phases, which has long been ignored in studies on nanofluidic motions, can be a dominant factor. In a nanotube, the gas solubility is no longer a material constant; rather, it is highly dependent on the characteristic length scale and significantly affects the liquid motion.

Results and Discussion

Atomistic Study of the Gas−Liquid−Solid Interactions in a Nanoenvironment. CNTs with varying radii are employed as model nanoenvironments to explore the fundamental size effects of nanofluidic behaviors, without introducing additional parameters such as pore surface features. Insights of effective gas solubility were obtained by studying a cluster of 12 carbon dioxide (CO_2) molecules[8] in water confined by CNTs of four different radii. The CO_2 cluster was placed in the middle of a long open-ended tube and surrounded by water molecules, and the MD simulations were carried out at a constant temperature (300 K) with a constant pressure of 10 MPa for 20 ps, by using a condensed-phased optimized molecular potential for atomistic simulation studies.[9] The average distance between carbon atoms in the nearest CO_2 molecules is plotted as a function of CNT radius in Figure 1, where the separation is considerably larger in larger tubes, indicating an easier solvation. In a small nanotube (e.g., (10,10)), the space is insufficient for the water molecules to surround and dissolve the CO_2 molecules, and thus the integrity of the CO_2 cluster remains, whereas in a relatively large pore (e.g., (40,40)), the CO_2 molecules were quickly dissolved in the water in a few picoseconds. That is, there is a critical pore size below which the solvation of CO_2 molecules becomes difficult. The observations hold at other pressures; thus, during the liquid infiltration into a small nanochannel with increasing pressure, the CO_2 cluster is likely to remain with high pressure and thus play an important role, whereas the CO_2 phase can be rapidly dissolved in a large tube and the solid−liquid interaction dominates the nanofluidic behavior. Note that, if the gas molecules cannot be entrapped, such as at a large solid surface or in a through-fluidic channel, the gas solubility would exhibit different characteristics as the length scale approaches the nanometer level.[5] Moreover, in the current study, the simulation time is insufficient to reveal the saturated liquid−gas mixture configurations, which have been discussed by a number of researchers.[6,10]

Inspired by the size effect of the gas solubility study, we investigated (10,10) and (40,40) CNTs to analyze the effect of gas phase on liquid infiltration and defiltration behaviors in a nanoenvironment. One end of the CNT was closed, providing a simplified boundary condition for either the end of a closed nanochannel or the symmetric compression of liquid and "gas phases" (CO_2 molecules) from both ends of a long nanochannel. Initially, the tube either was vacuumed or contained a certain number of CO_2 molecules, and its surface was assumed smooth.[11] The CNT length was chosen such that the end effect was negligible in the initial infiltration stage[12] (but it will become important at the final stage of infiltration and the initial stage of defiltration, when the entire pore is almost filled with water, discussed below). Depending on the tube size, the CNT was surrounded by several thousands of water molecules at a constant temperature (300 K) with an initial pressure of 0.1 MPa. By varying the size of the computational cell, the pressure variation in the system (up to 100 MPa in this study) was obtained through the bulk modulus of water (2.1 GPa). All pressure values referred in this study are that in the water phase. At any pressure, a normalized volume fraction of the infiltrated water molecules was calculated, which is defined as the number of H_2O molecules in the CNT divided by that at 100 MPa, both measured at 50 ps after quasi-equilibrium. In essence, the volume fraction indicates the infiltrated volume of liquid in the nanotube at a given pressure.

In a bulk water structure, a H_2O molecule has approximately four hydrogen bonds; however, a molecule adjacent to the open end of a CNT tends to lose one or two hydrogen bonds, thus having a higher energy level. Therefore, in the absence of other assistance (e.g., an external pressure), the H_2O molecules near the CNT open end must rely on random thermal vibrations to overcome the energy barrier to lose hydrogen bonds and to infiltrate into the hydrophobic CNT. When a (10,10) CNT was initially vacant, with the aid of pressure difference (at 78 MPa), H_2O molecules gradually diffused into the CNT and the normalized water volume was about 27% (Figure 2a). On the other hand, when the same CNT initially contained a single CO_2 molecule, due to the van der Waals attraction exerted by

(8) The carbon dioxide was chosen since its solubility in bulk water is high, which helps to accelerate simulation. The essential features were retained as nitrogen or oxygen was chosen.
(9) Sun, H.; Ren, P.; Fried, J. R. *Comput. Theor. Polym. Sci.* **1998**, *8*, 229.
(10) Huang, D. M.; Chandler, D. *J. Phys. Chem. B* **2002**, *106*, 2047.
(11) We also carried out MD simulations with silica tubes and a CNT with varying cross sections to better match the parallel experiments. Although different infiltration and defiltration rates were observed, similar gas-phase effects and tube radius effects were revealed.
(12) The interaction between the CNT atoms and water molecules is the van der Waals interaction, whose cutoff distance is about 1 nm. The effect of the CNT capped end on initial infiltration behavior is secondary as long as the tube (pore) length is much longer than 1 nm.

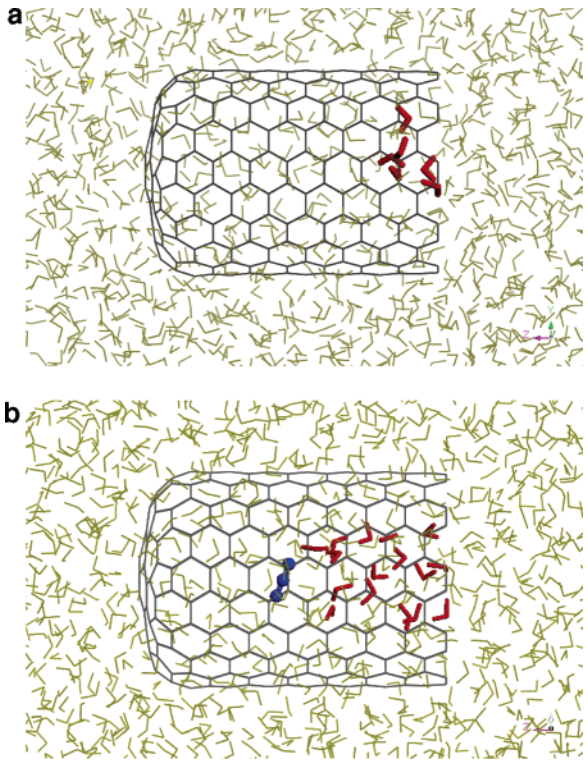

Figure 2. Water infiltration in (a) a vacant CNT and (b) a CNT with a single CO_2 molecule; both were taken at 50 ps after equilibrium. The infiltrated water molecules are red, and the CO_2 molecule is blue. The water molecules outside the CNT are gray.

the CO_2 molecule, under the same pressure the normalized water volume was 68% (Figure 2b), nearly 2.5 times larger. The effect of the CO_2 molecule on infiltration is obvious where the CO_2 molecule has helped the liquid to enter the nanotube. Note that in most previous MD studies on liquid motions in nanochannels,[2] this important effect was ignored, which would lead to an underestimation of the liquid infiltration rate.

The CO_2 molecules can also be critical to the defiltration process. In the MD simulation, a long one-end-capped (10,10) CNT that encompassed 10 CO_2 molecules was analyzed. Due to the dramatically decreased gas solubility in a small nanopore, when the pressure was increased, the infiltrated H_2O molecules pushed the CO_2 molecules toward the capped end to form a cluster (similar to the inset in Figure 1); meanwhile, the water pressure was increased continuously, leading to the entrance of more H_2O molecules, which stabilized at 100 MPa (Figure 3).

By comparing the total free energies of a CNT filled by water molecules and an empty CNT with the same amount of water molecules surrounding it, the effective excess CNT−water interfacial tension can be obtained as 58 mJ/m^2. According to the classic capillary theory, the infiltration pressure should be around 160 MPa, qualitatively fitting with the MD simulation result, indicating that the long-term structure of the ensemble is governed by thermodynamics. This was recently confirmed by continuum analyses,[13] mean-field models and simulations of nanofluidic properties,[14] as well as atomic simulations on saturated gas concentrations,[7] where unique nanometer-scale phase behaviors were revealed. However, since thermodynamic

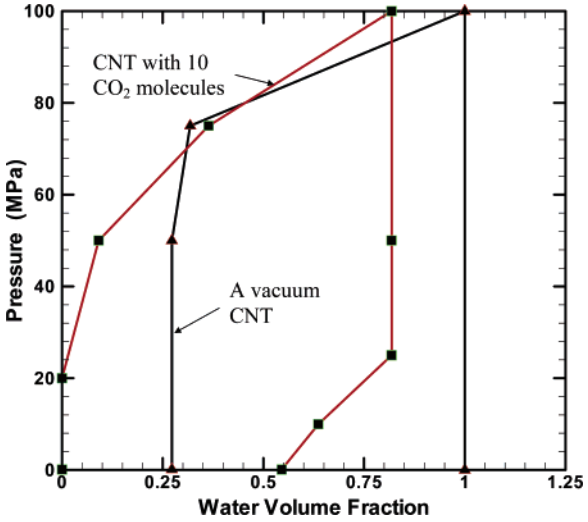

Figure 3. Sorption isotherm curves of a CNT obtained from MD simulation: with and without gas molecules.

models predicted reversible system performance, to capture the hysteresis of the infiltration−defiltration loop, kinetics of liquid−gas−solid interaction must be taken into consideration. In the current study, it was observed that upon unloading the water molecules were confined in the CNT until the pressure was lower than about 25 MPa, at which point the H_2O molecules began to "flow" out. In essence, at the defiltration pressure of 23 MPa in this simulation, the gas molecule cluster was able to repel the water molecules out. About one-third of the water molecules exited the nanochannel when the pressure was reduced to 1 bar. Note that a prerequisite for the formation of a gas molecule cluster is that the CNT diameter should be sufficiently small, less than a few nanometers.[15] Thus, the numerical analyses indicated that the defiltration is possible for relatively small nanopores and the trapped gas phase is the critical driving force, both in qualitative agreement with the experimental observations that will be discussed below.

By contrast, if the nanopore was relatively large, with increasing pressure the water molecules infiltrated into the nanopore and dissolved the CO_2 molecules (inset in Figure 1) and thereby filled the CNT volume at a sufficiently high pressure. The situation then became similar to that of Figure 2a where the CNT was initially vacant and the liquid−solid interaction dominates. To study the effect of CO_2 molecules on the liquid defiltration, in Figure 3 MD simulations for the same (10,10) CNT without and with CO_2 molecules were compared. In the absence of the CO_2 molecules, the normalized infiltrated water volume was about 27%; the number of the H_2O molecules inside the CNT remained constant until the pressure was increased to a critical value, at which point pressure-induced infiltration started to take place. The higher pressure lifted the system energy to the threshold of breaking roughly one-half of the hydrogen bonds for several H_2O molecules close to the tube

(13) (a) Evans, R.; Parry, A. O. *Phys. Condens. Matter* **1990**, *2*, 15. (b) Wennerstrom, H. *J. Phys. Chem. B* **2003**, *107*, 13772.

(14) (a) Han, A.; Kong, X.; Qiao, Y. *J. Appl. Phys.* **2006**, *100*, 014308. (b) Lefevre, B.; Saugey, A.; Barrat, J. L.; Bocquet, L.; Charlaix, E.; Gobin, P. F.; Vigier, G. *J. Chem. Phys.* **2004**, *120*, 4927. (c) Yushchenko, V. S.; Yaminsky, V. V.; Shchukin, E. D. *J. Colloid Interface Sci.* **1983**, *96*, 307. (d) Lum, K.; Chandler, D. *Int. J. Thermophys.* **1998**, *19*, 845. (e) Leung, K.; Luzar, A.; Bratko, D. *Phys. Rev. Lett.* **2003**, *90*, 065502. (f) Luzar, A. *J. Phys. Chem. B* **2004**, *108*, 19859.

(15) The value can be estimated by adding the size of gas and liquid molecules, and the van der Waals equilibrium distances between the gas/liquid and liquid/solid molecules.

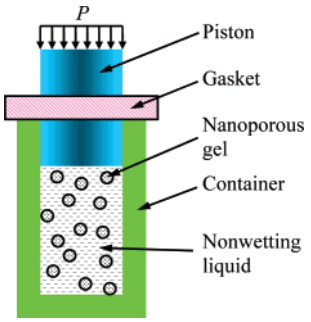

Figure 4. Schematic diagram of the experimental setup. By compressing the piston into the container, the liquid can be forced into the hydrophobic nanoporous silica gel. As the pressure is reduced, the confined liquid may or may not come out of the nanopores, depending on the gas content in the nanoenvironment and the nanopore size.

opening. Subsequently, more H_2O molecules could enter the CNT and the infiltration took place when the pressure was between 78 and 100 MPa (saturation). The infiltration pressure was thus determined to be about 80 MPa. Upon removing the external pressure, all of the H_2O molecules were "locked" inside the CNT, since, after the H_2O entered into the CNT, new hydrogen bonds were generated and the H_2O molecules had a more favorable energy level. In addition, a van der Waals attraction existed between the CNT wall and the infiltrated H_2O molecules. Thus, the numerical simulation predicted that "nonoutflow" is possible for either small nanopores without gas molecules trapped inside or large nanopores where the gas phases were dissolved in water.

Experiment on Nanoporous Materials. To validate the MD simulation results of the gas-phase effect on nanofluidic behaviors, a pressure-induced infiltration experiment was performed on a hydrophobic nanoporous Fluka C_8 end-capped silica gel of average pore size of $r = 7.8$ nm and standard deviation of 2.4 nm. At the first-order approximation level where the solid−liquid interaction was characterized by a single parameter of effective interface tension, it could be employed as an "analogue" to the CNTs, even though the details of its pore surface features were abundantly different. The specific surface area of the silica gel was 287 m^2/g, and the particle size was 15−35 μm.[16] Initially, 0.5 g of the nanoporous silica gel was immersed in 7 g of 15 wt % aqueous solution of sodium chloride and sealed in a polymethyl methacrylate container, as depicted in Figure 4. The nanopores of the silica gel were of a three-dimensional structure, which has been discussed by Polarz and Smarsly.[17] The sodium chloride was added to improve the gas solubility, so that the phenomena predicted in the MD simulation could be more pronounced. The addition of sodium chloride might increase the complexity of liquid behaviors in nanopores, the details of which are still under investigation. Nevertheless, the major characteristics of infiltration and defiltration were not affected.[1]

By using a type 5569 Instron machine, immediately prior to the infiltration−defiltration experiment, a preloading cycle was applied so as to deactivate the inaccessible pores, with crosshead speed of 0.5 mm/min and maximum pressure of 40 MPa. The air bubbles in between the silica particles were removed by using a Branson 200 ultrasonic machine before the test. Note that a

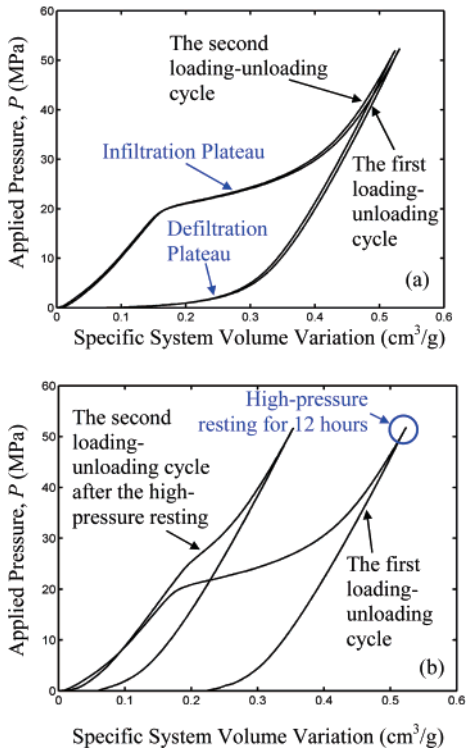

Figure 5. Sorption isotherm curves of the C_8 reversed-phase silica gel: (a) subjected to a cyclic loading and (b) with high-pressure resting. The curves have been moved along the horizontal axis. During the high-pressure resting, the gas molecules in the nanopores diffused out, which led to the "nonoutflow", indicating that the presence of gas molecules in the nanopores is critical to the defiltration process.

significant amount of gas molecules was entrapped in the nanopores.[18] As the piston was compressed into the container, the piston displacement, d, and the force acting on the piston, F, could be continuously measured. We denoted $A = 286$ mm^2 as the cross-sectional area of the piston. The applied pressure was calculated as $P = F/A$, and the specific system volume change was defined as $\Delta V = d \cdot A/m$, with m being the mass of the nanoporous silica gel. When the pressure was low, water could not enter the hydrophobic nanopores, resulting in a relatively linear $P - \Delta V$ relationship with the slope close to the bulk modulus of water. When the pressure was higher than the critical value of 17 MPa, water could be forced into the nanopores as the energy barrier associated with the capillary effect was overcome, leading to the prominent infiltration plateau of the sorption isotherm curve, as shown in Figure 5a. The infiltration process was completed when the pressure was 27 MPa. As the applied load was reduced, after the initial linear unloading, the confined liquid came out of the nanopores, forming the defiltration plateau. When the applied pressure was reduced to zero, most of the nanopore volume had been recovered, and therefore, as the loading−unloading cycle was repeated the sorption isotherm curve was nearly the same as the first loop. During the infiltration and defiltration process, the liquid phase was clear and no air bubble could be detected, indicating that the gas phase in the nanopores remained confined.[19]

(16) The gas absorption analysis was performed at Quantachrome Instruments, Boynton Beach, FL.
(17) Polarz, S.; Smarsly, B. *J. Nanosci. Nanotechnol.* **2002**, *2*, 581.
(18) Dabrowski, A. *Adv. Colloid Interface Sci.* **2001**, *93*, 135.
(19) (a) Fadeev, A.; Eroshenko, V. *J. Colloid Interface Sci.* **1997**, *187*, 275. (b) Kong, X.; Qiao, Y. *Philos. Mag. Lett.* **2005**, *85*, 331.

The excess gas molecules in the nanopores could be removed through room-temperature diffusion. After the pressure-induced infiltration, if the peak pressure was maintained at 50 MPa for 12 h, the confined liquid would remain in the nanopores. Initially, due to the gradual dissolution of the entrapped gas, the gas concentration inside the nanoporous silica gel was higher than that outside, while over time an equilibrium condition would be reached under hydrostatic pressure. As a result, the gas molecules diffused from the nanopore and a large number of air bubbles of average size of about 0.1 mm appeared. Under this condition, as the applied pressure was subsequently reduced to zero, little defiltration could be observed and therefore the defiltration plateau was quite unclear, as shown in Figure 5b. That is, most water remained in the nanopores, which could also be verified from the second loading cycle where very few water molecules could enter the nanopores (i.e., the infiltration plateau was much narrower compared with that of the first loading). Under the atmosphere pressure, the total volume of air bubbles appearing after the high-pressure resting, normalized by the mass of silica gel, was about 0.35 cm^3/g, smaller than but close to the accessible nanopore volume. Clearly, during the holding at peak pressure, the reduction in gas concentration in nanopores significantly enhanced the confinement effect of pore walls and resulted in the "nonoutflow" of the confined liquid. In other words, the gas phase inside the nanopores provided a critical driving force of defiltration, the absence of which would cause difficulties of liquid motion, as predicted by the MD simulation.[21]

In a comparison experiment on a Fluka C_{18} end-capped silica gel immersed in water, it was confirmed that, in addition to the gas content, the defiltration process was also affected by the pore size. The average pore size of the silica gel was 22 nm, with the standard deviation of 5.7 nm. The experimental procedure were kept the same as that of the C_8 end-capped silica. It was observed that, no matter whether the high-pressure resting was performed, the "outflow" was negligible. After the high-pressure resting, the total volume of air bubbles was close to the accessible nanopore volume (i.e., the gas diffusion characteristics were quite insensitive to the nanopore size). Note that while a few conventional porosimetry theories such as the change in effective contact angle and the "ink-bottle" effect of pore walls could relate the liquid behaviors to the pore size,[20] the gas-phase effect is pronounced only when the pore diameter is comparable with gas molecular size and should be explained by the MD simulations.[21]

Conclusion

To summarize, while the nominal gas molecule density is lower than that of liquids by orders of magnitude, the influence of gas molecules on liquid infiltration and defiltration in confining nanoenvironments can be significant, and ignoring it can be questionable. The MD simulation of nanotubes not only shows the dependence of the defiltration behavior on the pore size and the pore surface properties, but also reveals the inherent interactions between gas and liquid phases, where the effective gas solubility highly depends on the characteristic length scale. In a nanochannel, even a single gas molecule can significantly promote the liquid infiltration and may make the confined liquid unstable. The low effective gas solubility in a small nanochannel leads to the formation of trapped gas clusters during infiltration and the outflow behavior during defiltration, whereas the liquid−solid interaction is dominant after the gas phase is dissolved in larger nanopores or after the gas phase is diffused out of small nanopores, causing the nonoutflow phenomenon. Note that the current experimental work is only loosely related to the MD simulations. It shows analogous liquid behaviors but does not provide a quantitative validation of the numerical results. More work is in progress to better match simulation with experiment, with system parameters such as the pore surface features and coverage being incorporated, and to deduce the quantitative contribution of gas effect on infiltration and defiltration in selected systems. Since gas entrapment in nanopores and nanotubes is almost inevitable in practice, for analyses of nanofluidic motions its effect must be carefully taken into consideration.

Note Added after ASAP Publication: Additional text changes and a revised Acknowledgment were received since this posted ASAP on February 6, 2007; the corrected version posted on February 7, 2007.

Acknowledgment. The numerical study was supported by the National Science Foundation under Grant No. CMS-0407743 and CMS-0643726. The discussion and the pressure induced infiltration experiment were supported by the Army Research Office under Grant No. W911NF-05-1-0288.

JA067185F

(20) *Nanoporous Materials: Science and Engineering*; Lu, G. Q., Zhao, X. S., Eds.; Imperial College Press: London, 2004.

(21) The aforementioned behaviors were observed in all nanoporous systems that we have tested with distinct average pore sizes. In the present study, although pore surface features and coatings of C_8 and C_{18} silicas are somewhat different, they should not lead to the observed fundamental difference in the sorption isotherm curves.